NANO LETTERS

Letter

pubs.acs.org/NanoLett

Dynamics of Four-Photon Photoluminescence in Gold Nanoantennas

Paolo Biagioni,*[,†] Daniele Brida,[‡] Jer-Shing Huang,[§] Johannes Kern,[∥] Lamberto Duò,[†] Bert Hecht,[∥] Marco Finazzi,[†] and Giulio Cerullo[‡]

[†]CNISM and [‡]IFN - CNR - Dipartimento di Fisica, Politecnico di Milano, Piazza Leonardo da Vinci 32, 20133 Milano, Italy

[§]Department of Chemistry and Frontier Research Center on Fundamental and Applied Sciences of Matters, National Tsing Hua University, Hsinchu 30013, Taiwan

[∥]Nano-Optics and Bio-Photonics Group, Experimentelle Physik 5, Physikalisches Institut, Wilhelm-Conrad-Röngten-Center for Complex Material Systems, Universität Würzburg, Am Hubland, 97074 Würzburg, Germany

Supporting Information

ABSTRACT: Two-pulse correlation is employed to investigate the temporal dynamics of both two-photon photoluminescence (2PPL) and four-photon photoluminescence (4PPL) in resonant and nonresonant nanoantennas excited at a wavelength of 800 nm. Both 2PPL and 4PPL data are consistent with the same two-step model already established for 2PPL, implying that the first excitation step in 4PPL is a three-photon sp → sp direct interband transition. Considering energy and parity conservation, we also explain why 4PPL behavior is favored over, for example, three- and five-photon photoluminescence in the power range below the damage threshold of our antennas. Since sizable 4PPL requires larger peak intensities of the local field, we are able to select either 2PPL or 4PPL in the same gold nanoantennas by choosing a suitable laser pulse duration. We thus provide a first consistent model for the understanding of multiphoton photoluminescence generation in gold nanoantennas, opening new perspectives for applications ranging from the characterization of plasmonic resonances to biomedical imaging.

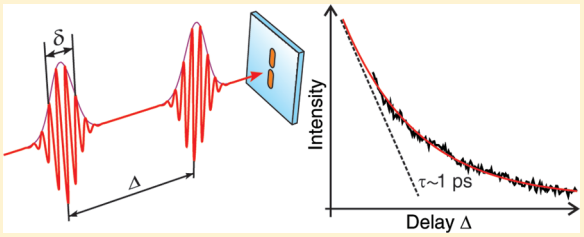

KEYWORDS: *Plasmonics, two-photon photoluminescence, four-photon photoluminescence, gold nanoantennas*

Noble-metal nanoparticles and nanoantennas are attracting an ever increasing attention since the resonant behavior of the electron plasma oscillations in response to the external optical field enables numerous spectroscopic and sensing applications.[1,2] The large near-field peak intensity enhancement that accompanies such resonances can give rise to a whole range of nonlinear optical effects. In this context, two-photon photoluminescence (2PPL) imaging has become one of the preferred tools to study modal patterns of plasmonic resonances, especially in gold.[3−7] Two-photon absorption has also established gold nanoparticles among the most promising theragnostic biomarkers, since they provide at the same time the possibility for deep tissue imaging as well as for local heating in photothermal therapies.[8−10]

At variance with coherent 2PPL in molecules, which usually proceeds through a virtual intermediate state, it has been proposed[11] and experimentally demonstrated[12] that 2PPL in gold is the result of two sequential single-photon absorption steps mediated by a real state. In detail, the first photon excites an electron via an intraband transition within the sp conduction band, while the second photon excites an electron from the d band to recombine with an sp hole in the conduction band. The dynamics of the TPPL signal, caused by the radiative recombination of d holes, is ruled by the relaxation time of the transient distribution excited in the sp conduction band after the first absorption event. Because of the increased density of states, interband radiative recombination in 2PPL occurs close to the L and X points in the reciprocal space, leading to two emission bands located in the green and red spectral regions, respectively.[11] Higher-order absorption processes with characteristic power dependence have also been reported in the literature. Three-photon absorption has been observed from single gold nanoparticles,[13] while four-photon photoluminescence (4PPL) has been reported for resonant gold dipole antennas.[4] Interestingly, in the case of 4PPL, an increased spectral weight of the green (L point) emission band was observed, compared to standard 2PPL.[4] While the mechanism behind 2PPL is well understood, there is no consistent model for the observed higher-order nonlinearities and the appearance of either order in experiments seems to be elusively random.

Here, we study the photoluminescence (PL) dynamics of both a rough gold film as well as high-quality resonant single-crystalline nanoantennas.[14] While the rough gold film only shows 2PPL, for the nanoantennas we observe both 2PPL and 4PPL depending on the pulse length. In order to characterize the nonequilibrium dynamics of both 2PPL and 4PPL, we perform two-pulse correlation measurements using sub-100 fs pulses centered at 800 nm in which PL is recorded as a function

Received: February 14, 2012
Revised: April 27, 2012
Published: May 2, 2012

   dx.doi.org/10.1021/nl300616s | *Nano Lett.* 2012, 12, 2941−2947

of the time delay between two pulse replicas.[15,16] For both 2PPL and 4PPL, two-pulse correlation shows a single-exponential incoherent tail that directly probes the 1 ps relaxation time of the nonequilibrium sp electron distribution, which therefore represents the intermediate excited configuration for both cases. On the basis of this observation and on the Au band structure, we suggest that in the case of 4PPL the intermediate nonequilibrium sp distribution is created by a coherent three-photon transition mediated by virtual states, as implied by energy and parity conservation and supported by the experimental features of the 4PPL spectra. In the framework of our model, the occurrence of orders other than 2 and 4 should be hindered for the 800 nm excitation wavelength. We provide further evidence for the validity of this picture by demonstrating control over the occurrence of 4PPL versus 2PPL from the same resonant nanostructure by changing the pulse duration for a given average power. In addition, we also find that the relaxation time of the intermediate hot electron distribution is shortened in the particular case of resonant optical antennas as compared to off-resonance antennas. Possible explanations for this intriguing behavior are discussed.

The experimental setup is based on a commercial confocal microscope (Alpha-SNOM, WITec GmbH, Germany) coupled to a mode-locked Ti:sapphire oscillator producing 40 fs pulses at 100 MHz repetition rate and 800 nm wavelength. Collinear pulse pairs with computer-controlled delay Δ (see sketch in Figure 1a) are generated by a balanced Michelson interferometer. The output of the interferometer is coupled into a short piece of single-mode fiber, whose far end serves as a pointlike source for the confocal microscope. Light is focused onto the sample by an oil-immersion objective with 1.4 numerical aperture. Precompensation of dispersion introduced by the optics in the beam path is achieved by a double pass in a pair of SF10 Brewster-cut prisms. After optimization of the precompensation stage, a pulse duration $\delta < 100$ fs is obtained after the objective, as measured with second-harmonic generation (SHG) correlation from a thin β-barium borate (BBO) crystal. Gold PL is collected using the same objective and sent to a photon counter through a multimode fiber whose 75 μm core also acts as a collection pinhole for background rejection. Suitable spectral filters (transmission window 450–750 nm) are inserted in the collection path in order to selectively detect the gold PL while completely rejecting both the fundamental excitation wavelength and possible second-harmonic signals. A photoncounting photomultiplier tube is used for PL detection.

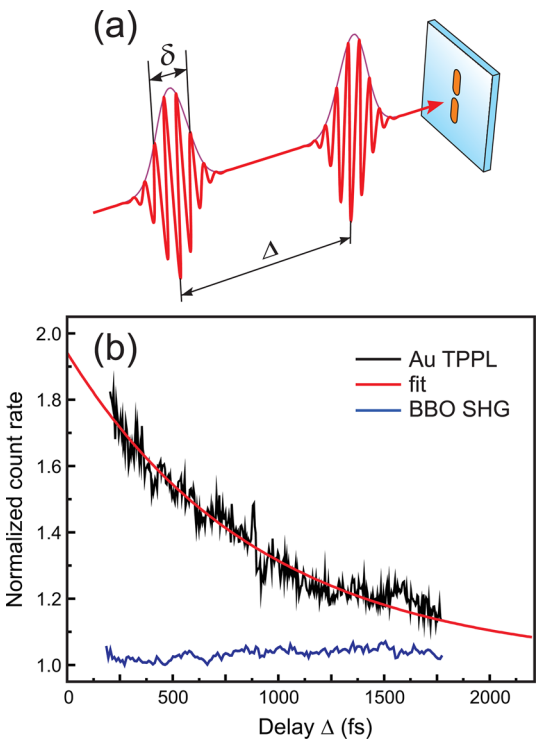

Figure 1. (a) Sketch of the two-pulse correlation measurements on gold nanoantennas; (b) tail of the correlation curve (black line) for the 2PPL signal from a rough gold film. The red line is a best fit according to eq 2 (see text) with τ_{sp} as the only free parameter. The blue trace corresponds to the reference SHG correlation signal obtained from a BBO crystal placed at the sample position. The count rates are normalized to those obtained with two laser pulses separated by a time delay $\Delta \sim 4$ ps.

In order to record a two-pulse PL correlation curve, the area of interest is first imaged by means of scanning confocal optical microscopy (see Supporting Information, Figure 1), then a selected structure is positioned in the focus and the PL signal is recorded as a function of the pulse delay Δ. The typical average excitation power needed to obtain a sizable correlation signal without damaging the sample is of the order of 100 μW. Count rates are normalized to those obtained with two well-separated laser pulses (time delay $\Delta \sim 4$ ps). We generally observe that the 2PPL or 4PPL signals of continuously illuminated single- or multicrystalline gold structures show intensity fluctuations, which are the main source of noise in the experiments.[17]

We first investigate a reference sample for 2PPL, that is, a rough polycrystalline gold film (~50 nm thickness) fabricated by thermal evaporation.[3] The corresponding 2PPL correlation trace is shown in Figure 1b for delay times $\Delta > 200$ fs, revealing an ~1 ps exponential tail. Comparison with the SHG correlation curve acquired replacing the gold film by a BBO crystal (blue line in Figure 1b) confirms that this tail is indeed due to gold 2PPL dynamics and not to a residual chirp of the light pulses.

The observed ~1 ps dynamics is in full agreement with previous experimental results where the 2PPL yield was measured as a function of the pulse duration and the same limiting dynamics was observed.[12] In order to understand this result, let us recall that gold 2PPL in the recorded spectral range is mostly generated by the recombination of holes in the 5d band created via a two-step process involving two sequential one-photon absorption transitions.[11,12] This excited hole distribution can relax radiatively and directly contribute to 2PPL, albeit with a small quantum yield. It can also recombine nonradiatively within the sp band by generating localized plasmon oscillations that subsequently radiate, increasing the luminescence quantum yield.[18,19]

The two sequential one-photon absorption events are governed by the following rate equations[12]

$$\frac{dN_{sp}}{dt} = \sigma_{sp\rightarrow sp} N F(t) - \frac{N_{sp}}{\tau_{sp}} - \sigma_{d\rightarrow sp} N_{sp} F(t) \quad (1a)$$

$$\frac{dN_{d}}{dt} = \sigma_{d\rightarrow sp} N_{sp} F(t) - \frac{N_{d}}{\tau_{d}} \quad (1b)$$

where N is the sample density expressed as atoms per unit volume, N_{sp} and N_d are the densities of holes created below the

dx.doi.org/10.1021/nl300616s | Nano Lett. 2012, 12, 2941–2947

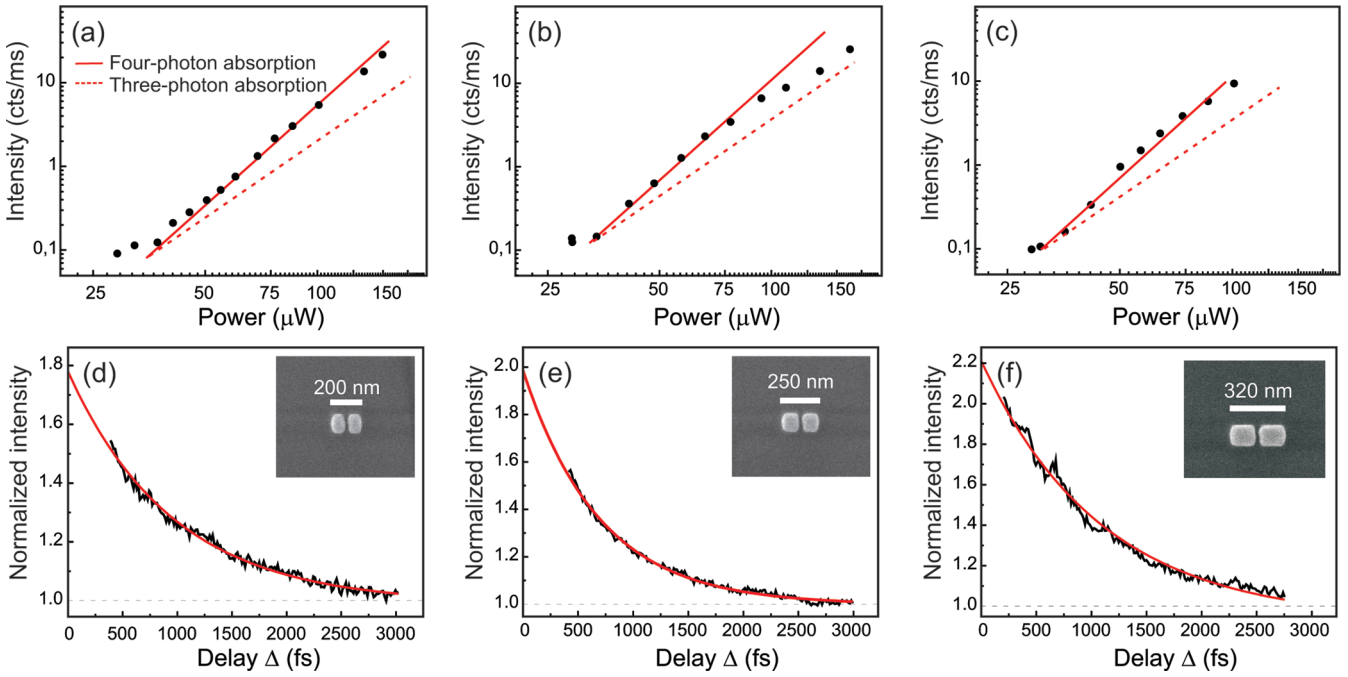

Figure 2. 4PPL power curves (a–c) and normalized correlation curves (d–f) for three different nanoantennas characterized by different arm lengths but an otherwise similar geometry. Red solid (dashed) lines in the power curves represent a guide for four-photon (three-photon) behavior. The correlation data are obtained with 50 μW average excitation power per arm in the interferometer and then normalized to the count rate obtained with the two laser pulses separated by a time delay $\Delta \sim 4$ ps. Insets are scanning electron microscopy images of the antennas. The red lines in panels (d), (e), and (f) are best fits obtained by using the function from eq 2 (see text).

Fermi level in the sp and d bands, respectively, while τ_{sp} and τ_d represent the relaxation times of the sp and d holes. $F(t)$ describes the pulse intensity profile used for the excitation and $\sigma_{sp\rightarrow sp}$ ($\sigma_{d\rightarrow sp}$) is the cross section of the sp → sp (d → sp) transition excited by the first (second) absorbed photon. The third term on the right-hand side of eq 1a is negligible in the small perturbation regime characterized by $N_{sp} \ll N$.

The 2PPL intensity $I_{2PPL}(\Delta)$ can be obtained from eq 1 by calculating the temporal average value $\langle N_d \rangle$ to which the time-integrated PL signal is proportional.[12] To do this, we consider a function $F(t)$ consisting of two identical light pulses of duration δ separated by a time delay Δ. As already proposed in ref 12, the dynamics of the process is governed by τ_{sp}, which is typically on the order of 1 ps in gold.[12,20,21] Since the duration δ of the pulse impinging on the sample is below 100 fs, that is, much shorter than τ_{sp}, we obtain for the 2PPL intensity the following simple expression for delays $\Delta \gg \delta$

$$I_{2PPL}(\Delta) \propto \langle N_d \rangle \propto I_0^2(1 + e^{-|\Delta|/\tau_{sp}}) \qquad (2)$$

where I_0 is the time-averaged excitation intensity at the sample. Equation 2 correctly reproduces the experimentally found exponential dependence of the 2PPL count rate on the time delay Δ. The validity of eq 2 is independent of details of the laser pulses such as bandwidth and chirp, as long as $\delta \ll \tau_{sp}$ and $\delta \ll \Delta$. By fitting the experimental traces using eq 2 (red line in Figure 1b), we find $\tau_{sp} \sim 910$ fs, which is in good agreement with the typical relaxation times observed for electrons and holes close to the Fermi level in gold films and nanostructures due to electron–phonon interactions.[12,20,21]

We shall now discuss 4PPL correlation data obtained from gold nanoantennas. Antennas are prepared by focused ion-beam milling starting from single-crystalline gold flakes on an ITO-coated glass substrate.[14] Figure 2a–c reports the PL intensity as a function of the average excitation power for three gold dipole antennas with the same 10 nm gap and total lengths of 200, 250, and 320 nm, respectively (see SEM images in the insets of Figure 2d–f), measured by using pulses from one arm of the interferometer only. The slope of the power curves in a log–log plot (Figure 2a–c) clearly reveals a four-photon process. Noticeably, at variance with previous observations on multicrystalline nanoantennas,[4] in the sample under study 4PPL dominates over other multiphoton absorption orders (including 2PPL) over the whole investigated range of excitation powers, which is the one commonly used for nonlinear confocal microscopy on plasmonic nanoantennas. We tentatively attribute this behavior to the smaller gaps and better quality of resonances afforded by single-crystalline nanoantennas,[14] as well as to the sub-100 fs laser pulses employed in the experiment. The 250 nm long antenna shows a small deviation from slope of four for average powers higher than about 100 μW (Figure 2b), which can be attributed to thermal effects, as we discuss below. Confocal 4PPL maps and finite-difference time-domain (FDTD) simulations (see Supporting Information, Figure 1 and Figure 2a) show that the latter antenna is on resonance with the excitation wavelength. Indeed, in the experiment it provides the highest 4PPL count rate for a given excitation power in the confocal maps. Moreover, simulations show that upon illumination at a wavelength of 800 nm with a diffraction-limited spot it exhibits a local field intensity enhancement which is about a factor of 2–3 larger than those of the other two antennas. It is important to note that all antennas display single-exponential tails in the correlation curves (as shown in Figure 2d–f) that are remarkably similar to those exhibited by the multicrystalline gold film solely showing 2PPL (Figure 1b).

This observation unravels a universal behavior of the dynamics of the 4PPL processes. In particular, it suggests

dx.doi.org/10.1021/nl300616s | Nano Lett. 2012, 12, 2941–2947

that, irrespectively of the process order (two- or four-photon), the limiting intermediate step in the overall multiphoton cascade is always constituted by the same nonequilibrium Fermi distribution of sp holes, which relaxes with a ~1 ps time constant, as already found for standard 2PPL in gold.[12] The 4PPL correlation and power curves can be reproduced by the following model. We assume that the d holes, whose radiative recombination produces the PL in a n-order process, are generated by a cascade of n sequential absorption processes, each described by the following rate equation

$$\frac{dN_i}{dt} = \sigma_i N_{i-1}(t)F(t) - \frac{N_i(t)}{\tau_i} \quad (3)$$

where τ_i and N_i are the relaxation time and the density of holes in the ith intermediate configuration, respectively, and σ_i is the cross section of the transition from the $(i-1)$th to the ith configuration. Again, we consider a small perturbation regime in which $N_i \ll N_{i-1}$. This corresponds to neglecting terms that depend on the hole occupancy of the ith level, except the one describing its own relaxation, which is a valid assumption as long as the temperature of the Fermi gas remains small compared to the excitation photon energy. For the same reason, we also neglect terms that depend on occupancies of states at higher energy and describe the creation of a hole in the ith level due to the decay of a hole from a higher level. The experimental validation of this assumption relies on the fact that any significant deviation from the perturbative regime would result in a departure from the slope-4 behavior in the curves of Figure 2a–c. While this might tentatively be the reason for the observed behavior of the resonant antenna at very large excitation powers, as mentioned before, our data generally confirm the validity of this assumption. The initial conditions are $N_0(0) = N$ and $N_i(0) = 0$ for $i = 1...n$. By solving this system of coupled equations in the $\delta \ll \Delta$ limit, one obtains

$$I_{MPPL}(\Delta) \propto \langle N_d \rangle = \langle N_n \rangle \propto I_0^n\left(1 + \sum_{i=1}^{n-1} e^{-|\Delta|/\tau_i}\right) \quad (4)$$

Here, each of the n steps can in principle be related to a number of events, including interband transitions,[22] intraband transitions,[3] or generation/annihiliation of plasmons.[18] In particular, nonlinear excitation of a sp hole can account for the additional steps leading from 2PPL to 4PPL. Such processes are well-known and currently employed in multiphoton photoemission experiments[23] and as a probe in photoemission electron microscopy to investigate local field enhancements in noble-metal nanostructures.[24,25] Remarkably, this model holds even when some of the transitions involve a virtual intermediate state, that is, when transitions in the cascade are excited by a coherent multiphoton absorption. In this case, the corresponding relaxation time τ_i in eq 3 is equal to zero.

For $n = 4$, eq 4 correctly reproduces the observed 4PPL power dependence. The single-exponential correlation tail observed also in the case of 4PPL, when compared to eq 4, suggests that the dynamics is still dominated by one intermediate distribution having a relaxation time of the order of ~1 ps and that all other intermediate configurations are characterized by a relaxation time τ_i much shorter than the investigated time window (i.e., shorter than about 100 fs). It should be noted here that the relaxation time of the final configuration, an excited d hole, has been measured to involve both a fast[26] (sub-100 fs) and a very slow[11] (~1 ns) component. However, this relaxation time only affects the yield of the PL process, while it plays no role in the intermediate dynamics probed by our two-pulse correlation traces.

Our model therefore confirms that the dynamics can be very similar for different multiphoton absorption orders since the same longer-lived intermediate configuration dominates the absorption cascade, whose order n is in any case revealed by the dependence of the PL intensity on the average excitation intensity (Figure 2a–c). The dynamics of the other absorption steps leading to $n > 2$ in 4PPL is confined within the first 100 fs that are not accessed in our investigation. On the basis of this interpretation, it is therefore expected that the yield of 4PPL strongly depends on the excitation pulse duration, as opposed to standard 2PPL.[12] In order to verify this prediction, we repeat the measurement of the absorption order in the investigated antennas by sending femtosecond pulses through a longer piece of optical fiber, leading to a pulse duration $\delta > 700$ fs. Remarkably, we observe a transition from 4PPL to 2PPL for the same antennas (see Figure 3).

In the following we propose a consistent picture to describe the absorption steps leading to 4PPL, which also explains why 4PPL excited with 800 nm wavelength dominates over alternative multiphoton processes. As a starting point, let us consider the first absorption step, which in the case of 2PPL is an intraband indirect transition within the sp band. We further assume that in the case of 4PPL this sp → sp transition involves absorption of more than one photon. In this case, it is reasonable to assume that this multiphoton transition will be vertical in the reciprocal space, since a cascade of indirect absorption events would be exceedingly unlikely. By close inspection of the gold band structure[27] in the proximity of the L and X points, it can be seen that the direct gap between adjacent sp bands is about 3 eV around the L point (see Figure 4) and about 6.5 eV around the X point. The onset of the joint density of states (JDOS) in gold is therefore near the L point of the reciprocal space. Since the sp bands above and below the Fermi level at L disperse very rapidly, direct transitions can occur only within a small volume of the reciprocal space close to L. Such energy-allowed transitions, involving 2, 3, or 4 photons, are sketched in Figure 4 for the photon energy employed in our experiments (1.55 eV), together with a possible indirect one-photon transition typical for 2PPL. It should however be noted that the two sp bands drawn in the figure have different parity character at the L point, and that multiphoton transitions couple states with the same (opposite) parity when the number of photons involved in the process is even (odd). Therefore, parity conservation suggests that three-photon sp → sp transitions are likely to be privileged with respect to two- or four-photon transitions.[28] Moreover, two-photon transitions occur at the very onset of the JDOS (along the L–W direction) and are therefore further hindered. Also, by inspection of the Au bands at L, one can immediately see that the energy differences corresponding to three- or four-photon sp → sp transitions are both higher than the energy of the Van Hove singularity at L, which corresponds to a local maximum in the JDOS. Therefore, the JDOS has to be lower for four-photon compared to three-photon transitions, adding further consistency to the hypothesis that four-photon transitions should be much less effective than three-photon transitions. This leads to the conclusion that a three-photon sp → sp transition followed by a single-photon d → sp absorption resulting in 4PPL should be much more efficient

dx.doi.org/10.1021/nl300616s | Nano Lett. 2012, 12, 2941–2947

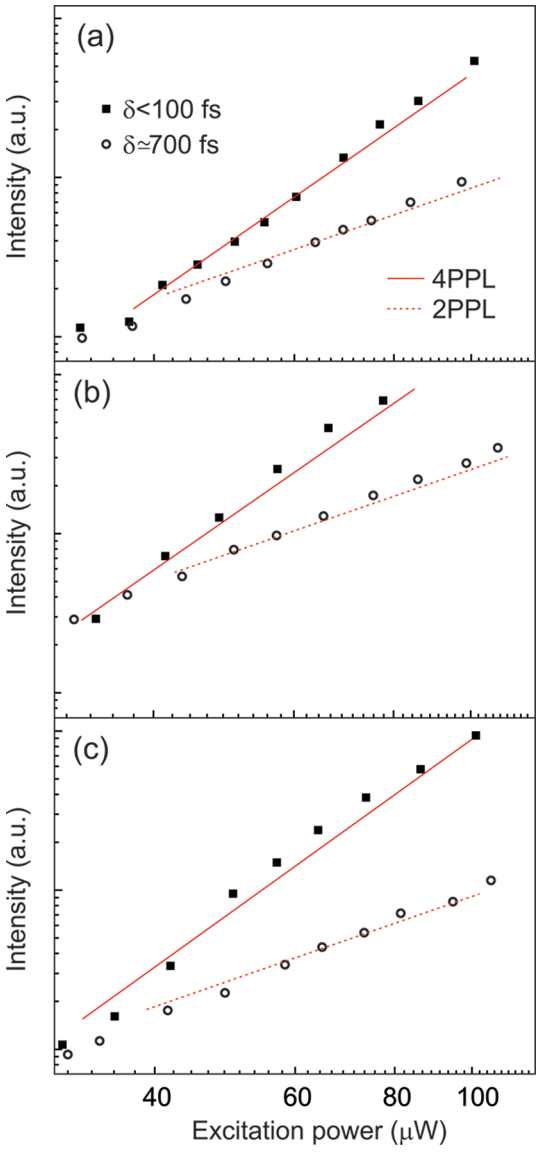

Figure 3. Comparison between the multiphoton emission curves for the three investigated antennas acquired with pulse durations δ < 100 fs and δ > 700 fs. The antenna length is (a) 200 nm, (b) 250 nm, and (c) 320 nm. Lines with slopes 2 (dashed) and 4 (solid) in the log–log plot are also shown as a guide for the eye.

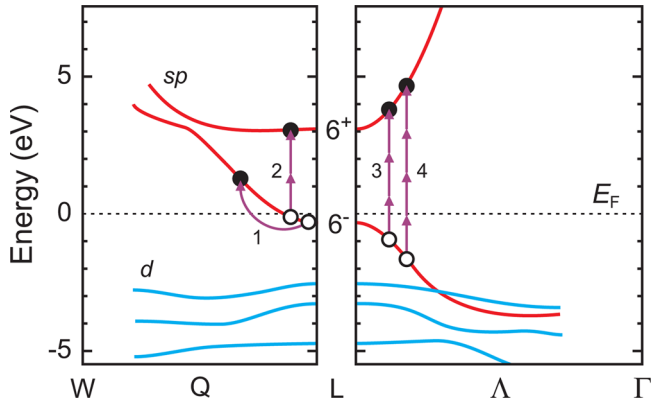

Figure 4. Gold relativistic band structure near the L point of the reciprocal space according to ref 27. Multiphoton direct sp → sp transitions are indicated by the vertical arrows. A bent arrow shows one of the possible indirect single-photon transitions. At the L point, the sp-derived states above and below the Fermi level respectively belong to the 6^+ (even) and 6^- (odd) irreducible representations of the D6d double group describing the symmetry properties of the reciprocal space at L.

than other multiphoton processes leading, for example, to three- or five-photon PL. Incidentally, we note here that even if a two-photon sp → sp transition would occur, this would create an sp hole close to the Fermi level (see Figure 4). Since the d band lies more than 2 eV below the Fermi level, this would require a two-photon d → sp transition to fill the energy distance between the d and the sp band, thus resulting again in 4PPL.

This proposed model is able to explain all experimental observations, including previous studies, concerning 4PPL from gold nanostructures.

(i) The three-photon sp → sp absorption step occurs through virtual levels (τ_i = 0) and is thus an instantaneous process, so that the relaxation time of the sp hole distribution solely determines the dynamics of the 4PPL process. The 2PPL and 4PPL two-pulse correlation experiments should thus display the same temporal behavior, as indeed observed in the experiments (see Figures 1 and 2).

(ii) The initial instantaneous three-photon absorption process in 4PPL should display a strong intensity dependence and its yield for a constant average excitation power, should scale as $1/\delta^2$; therefore, lengthening the excitation pulsewidth from 100 to 700 fs should reduce the 4PPL yield by a factor of ∼50. This is in agreement with the disappearance of 4PPL for the longer excitation pulses (see Figure 3).

(iii) At variance with 2PPL, 4PPL is the result of recombination processes occurring mainly at the L point of the reciprocal space. This is indeed fully consistent with the already mentioned increased spectral weight of the green emission (a signature of radiative d → sp recombination close to L) that was reported in ref 4 for antennas beyond the threshold for 4PPL.

These arguments do not completely rule out the possibility of observing PL power curves with intermediate slopes between those characteristic for 2PPL and 4PPL, as reported in the literature.[13,19] Such an intermediate behavior could be interpreted either as due to illumination conditions (power, pulse duration) exciting both 2PPL and 4PPL with similar efficiencies, or as a consequence of thermal effects,[29−31] which can cause saturation of the empty states above the Fermi level and increase electron–electron scattering, leading in both cases to a reduction of the PL yield.

Closer inspection of the fitting results for the correlation traces in Figure 2 reveals that the 250 nm resonant antenna actually displays a shorter relaxation time compared to the nonresonant ones. Indeed, the 200 and 320 nm antennas provide τ_{sp} ∼ 1000 ± 100 fs, which is in very good agreement with the results obtained for 2PPL in gold and with typical electron–phonon relaxation times, while for the resonant antenna we find τ_{sp} ∼ 650 ± 50 fs. Other measurements on nonresonant gold nanostructures all provide relaxation times similar to those found for 2PPL. Here we offer two possible explanations for this peculiar behavior:

(i) Because of the more efficient excitation of the resonant antenna, τ_{sp} might be reduced by thermal effects, leading

dx.doi.org/10.1021/nl300616s | Nano Lett. 2012, 12, 2941−2947

to smearing of the Fermi distribution function and thermally induced damping of the plasmon oscillation,[29−31] which is in agreement with the observed slight deviation from a pure four-photon behavior in Figure 2b.

(ii) A second intriguing possibility is that the intermediate excited sp-band electron distribution, required for 4PPL, efficiently decays into the resonant antenna plasmon modes.[18] This would represent a further loss channel directly contributing to a decrease in τ_{sp}.

In order to gain a qualitative insight into this second possibility, we have run FDTD simulations to calculate the enhancement in the total decay rate from an emitting dipole in the 800−1000 nm range (simulating intraband recombination)[3] coupled to the antenna feedgap (see Supporting Information, Figure 2b). We find that for the resonant antenna the enhancement in the decay rate (i.e., the antenna Purcell factor) is a factor of ∼10 larger than for the two nonresonant antennas therefore providing a possible explanation for the differences in τ_{sp} between resonant and off-resonance antennas.

In conclusion, we have analyzed the multiphoton PL dynamics in gap nanoantennas by performing two-pulse correlation experiments. By exploiting the large near-field intensity enhancement afforded by the antennas, we have observed 4PPL for which the temporal dynamics is dominated by the same ∼1 ps relaxation time as in the case of 2PPL. The two processes hold therefore strong similarities, since their dynamics is always limited by carrier relaxation in the sp band, and accordingly they proceed via the same intermediate configuration. Further absorption steps that increase the process order from $n = 2$ to $n = 4$ all happen within the first 100 fs, that is, at time scales shorter than the investigated time window, and as such they are more sensitive to the actual pulse duration in the sub-picosecond regime. Indeed, we also demonstrate that for the same nanoantennas 2PPL is obtained instead of 4PPL when the pulse duration is increased from $\delta < 100$ fs to $\delta \sim 700$ fs for the same average power. Therefore the 4PPL yield in gold, as opposed to the yield of 2PPL,[12] is strongly dependent on the pulse duration used for excitation, providing a handle for switching between 2PPL and 4PPL. High-quality single-crystalline nanoantennas were needed for the investigation since they reliably provide the local field enhancement in order to boost such nonlinear processes.[14] On the basis of our observations, we provide a first consistent framework for the explanation of 4PPL, where a three-photon direct transition between different sp bands is followed by a one-photon transition between the d and sp bands. Interestingly, a shortened relaxation time has been found for the resonant nanoantenna, which is attributed either to thermal effects or to the resonant decay of the intermediate excited distribution into the plasmon antenna mode.

■ ASSOCIATED CONTENT

Supporting Information

Figure 1: confocal 4PPL maps of the three investigated nanoantennas. Figure 2: (a) simulated field-intensity enhancement in the feed-gap of the investigated antennas; (b) results of FDTD simulations for an emitting dipole coupled to the antenna. This material is available free of charge via the Internet at http://pubs.acs.org.

■ AUTHOR INFORMATION

Corresponding Author

*E-mail: paolo.biagioni@polimi.it. Phone: +39 02 2399 6599. Fax: +39 02 2399 6126.

Notes

The authors declare no competing financial interest.

■ ACKNOWLEDGMENTS

The authors thank M. Savoini for insightful discussions and for his help during the experiments. Financial support from DFG (SPP 1391 "Ultrafast Nano-optics"), from National Science Council of Taiwan (NSC 99-2113-M-007-020-MY2), from Fondazione Cariplo ("Engineering of optical nonlinearities in plasmonic metamaterials"), from MIUR (PRIN Project No. 2008J858Y7), and from the European Union Nano Sci-European Research Associates ("FENOMENA") is gratefully acknowledged.

■ REFERENCES

(1) Biagioni, P.; Huang, J.-S.; Hecht, B. *Rep. Prog. Phys.* **2012**, *75*, 024402.

(2) Novotny, L.; van Hulst, N. *Nat. Photonics* **2011**, *5*, 83.

(3) Beversluis, M. R.; Bouhelier, A.; Novotny, L. *Phys. Rev. B* **2003**, *68*, 115433.

(4) Mühlschlegel, P.; Eisler, H.-J.; Martin, O. J. F.; Hecht, B.; Pohl, D. W. *Science* **2005**, *308*, 1607.

(5) Schuck, P. J.; Fromm, D. P.; Sundaramurthy, A.; Kino, G. S.; Moerner, W. E. *Phys. Rev. Lett.* **2005**, *94*, 017402.

(6) Ghenuche, P.; Cherukulappurath, S.; Taminiau, T. H.; van Hulst, N. F.; Quidant, R. *Phys. Rev. Lett.* **2008**, *101*, 116805.

(7) Huang, J.-S.; Kern, J.; Geisler, P.; Weinmann, P.; Kamp, M.; Forchel, A.; Biagioni, P.; Hecht, B. *Nano Lett.* **2010**, *10*, 2105.

(8) Nagesha, D.; Laevsky, G. S.; Lampton, P.; Banyall, R.; Warner, C.; DiMarzio, C.; Sridhar, S. *Int. J. Nanomed.* **2007**, *2*, 813.

(9) Durr, N. J.; Larson, T.; Smith, D. K.; Korgel, B. A.; Sokolov, K.; Ben-Yakar, A. *Nano Lett.* **2007**, *7*, 941.

(10) Gobin, A. M.; Lee, M. H.; Halas, N. J.; James, W. D.; Drezek, R. A.; West, J. L. *Nano Lett.* **2007**, *7*, 1929.

(11) Imura, K.; Nagahara, T.; Okamoto, H. *J. Phys. Chem. B* **2005**, *109*, 13214.

(12) Biagioni, P.; Celebrano, M.; Savoini, M.; Grancini, G.; Brida, D.; Mátéfi-Tempfli, S.; Mátéfi-Tempfli, M.; Duò, L.; Hecht, B.; Cerullo, G.; Finazzi, M. *Phys. Rev. B* **2009**, *80*, 045411.

(13) Farrer, R. A.; Butterfield, F. L.; Chen, V. W.; Fourkas, J. T. *Nano Lett.* **2005**, *5*, 1139.

(14) Huang, J.-S.; Callegari, V.; Geisler, P.; Brüning, C.; Kern, J.; Prangsma, J. C.; Wu, X.; Feichtner, T.; Ziegler, J.; Weinmann, P.; Kamp, M.; Forchel, A.; Biagioni, P.; Sennhauser, U.; Hecht, B. *Nature Comm.* **2010**, *1*, 150.

(15) Wang, X. Y.; Riffe, D. M.; Lee, Y.-S.; Downer, C. *Phys. Rev. B* **1994**, *50*, 8016.

(16) Lui, C. H.; Mak, K. F.; Shan, J.; Heinz, T. F. *Phys. Rev. Lett.* **2010**, *105*, 127404.

(17) Small fluctuations in the multiphoton intensity are plausibly related to very small modifications at the nanoscale, which however do not seem to introduce permanent changes in the yield and/or power dependence of the process and cannot be demonstrated even with accurate SEM imaging, or are caused by laser fluctuations.

(18) Dulkeith, E.; Niedereichholz, T.; Klar, T. A.; Feldmann, J.; von Plessen, G.; Gittins, D. I.; Mayya, K. S.; Caruso, F. *Phys. Rev. B* **2004**, *70*, 205424.

(19) Wissert, M. D.; Ilin, K. S.; Siegel, M.; Lemmer, U.; Eisler, H.-J. *Nano Lett.* **2010**, *10*, 4161.

(20) Sun, C.-K; Vallée, F.; Acioli, L. H.; Ippen, E. P.; Fujimoto, J. G. *Phys. Rev. B* **1994**, *50*, 15337.

(21) Groeneveld, R. H. M.; Sprik, R.; Lagendijk, A. *Phys. Rev. B* **1995**, *51*, 11433.
(22) Mooradian, A. *Phys. Rev. Lett.* **1969**, *22*, 185.
(23) Girardeau-Montaut, J. P.; Girardeau-Montaut, C. *Phys. Rev. B* **1995**, *51*, 13560.
(24) Aeschlimann, M.; Bauer, M.; Bayer, D.; Brixner, T.; Garcia de Abajo, F. J.; Pfeiffer, W.; Rohmer, M.; Spindler, Ch.; Steeb, F. *Nature* **2007**, *446*, 301.
(25) Douillard, L.; Charra, F.; Korczak, Z.; Bachelot, R.; Kostcheev, S.; Lerondel, G.; Adam, P.-M.; Royer, P. *Nano Lett.* **2008**, *8*, 935.
(26) Varnavski, O. P.; Mohamed, M. B.; El-Sayed, M. A.; Goodson, T., III *J. Phys. Chem. B* **2003**, *107*, 3101.
(27) Eckardt, H.; Fritsche, L.; Noffke, J. *J. Phys. F: Met. Phys.* **1984**, *14*, 97.
(28) Parity is a good quantum number only for the electron states at L, nevertheless two-, three-, and four-photon transitions can occur only very close to this point, where states are likely to maintain a well-defined parity.
(29) Rotenberg, N.; Bristow, A. D.; Pfeiffer, M.; Betz, M.; van Driel, H. M. *Phys. Rev. B* **2007**, *75*, 155426.
(30) Perner, M.; Bost, P.; Lemmer, U.; von Plessen, G.; Feldmann, J.; Becker, U.; Mennig, M.; Schmitt, M.; Schmidt, H. *Phys. Rev. Lett.* **1997**, *78*, 2192.
(31) Pelton, M.; Liu, M.; Park, S.; Scherer, N. F.; Guyot-Sionnest, P. *Phys. Rev. B* **2006**, *73*, 155419.